

Limits on Nonstandard Weak Currents from the Positron Decays of ^{14}O and ^{10}C

A. S. Carnoy, J. Deutsch, T. A. Girard,^(a) and R. Prieels

Institute de Physique Nucleaire, University Catholique de Louvain, 1348 Louvain-la-Neuve, Belgium

(Received 21 May 1990)

The relative polarization of positrons emitted in pure Fermi (^{14}O) and Gamow-Teller (^{10}C) decays has been measured using a new technique based on time-resolved positronium decay. The result $P_{\text{GT}}/P_{\text{F}} = 0.9996 \pm 0.0037$ provides constraints on possible right-handed and scalar-tensor current admixtures to the weak interaction of $-4 < \zeta\delta \times 10^4 < 7$ and $|(C_S/C_V) - (C_T/C_A)| = (1 \pm 9) \times 10^{-3}$ (90% C.L.), respectively.

PACS numbers: 23.40.Bw, 12.15.Ji, 24.70.+s, 27.20.+n

We report a comparison measurement of the longitudinal polarization (P) of positrons emitted in pure Fermi (F) and Gamow-Teller (GT) decays of ^{14}O and ^{10}C , respectively. Such comparisons are important in their ability to probe the standard-model structure of the electroweak interaction for the presence of additional contributions, such as right-handed charged weak currents¹ and scalar-tensor current admixtures to its predominantly $V-A$ description,² and to provide constraints complementary to other tests of the weak current helicity structure³ or to those deduced from the SN 1987A neutrino luminosity.⁴ In general, these contributions induce separate modifications to the standard pure F and GT polarization descriptions which in the absence of nuclear corrections result in $P_{\text{F}} = P_{\text{GT}}$. Their presence would be signaled by deviations of $R = P_{\text{F}}/P_{\text{GT}}$ from unity of order 0.1%.

The most precise such comparison to date, of 0.4% by the Groningen group using fourfold Bhabha polarimetry on the decays of $^{26}\text{Al}^m/^{30}\text{P}$, is however, considered by its authors to have reached its limits.⁵ Herein, an improved positronium-based technique^{6,7} is employed to yield a corroborative measurement in a factor of 3 less time. More significantly, the systematic errors have been carefully investigated to be a factor of 3 below the statistical, indicating the capability to pursue the measurement to a significantly improved precision.

The essentials of the polarimetry technique, based on observation of the time-resolved decay spectrum of the hyperfine positronium (Ps) formed by the nuclear-decay positrons in a strong magnetic field (B), have been described previously.^{6,7} This spectrum, as observed in our measurement, is shown in Fig. 1 (top), and consists of (a) a prompt peak corresponding to unresolved direct annihilation and perturbed singlet decay, (b) an intermediate perturbed triplet state, and (c) a long-lived unperturbed ($m = \pm 1$) triplet decay. The populations of the perturbed ($m = 0$) states depend on the relative direction of the perturbing field and the residual positron polarization (P). This feature is illustrated in Fig. 1 (bottom), where we show the ratio A of the decay spectra in the two opposing field directions (N_+/N_-). In the time re-

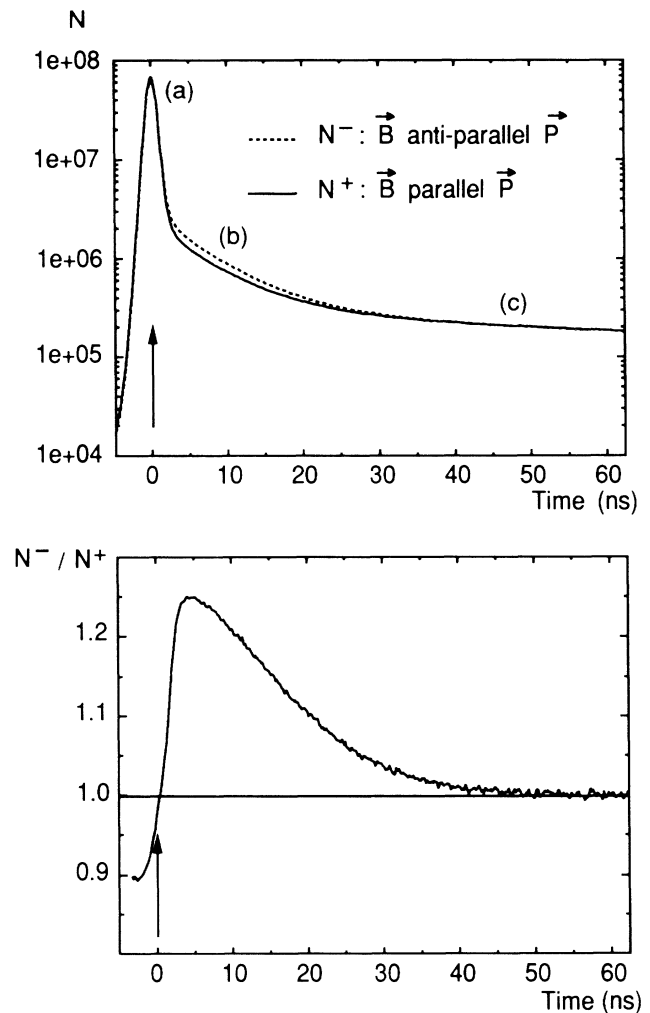


FIG. 1. Top panel: The experimental hyperfine Ps decay spectrum, showing (a) the unresolved direct annihilation and perturbed singlet, (b) triplet, and (c) unperturbed triplet components. The graph represents the integrated counts per channel (156 ps width) in window B of the measurement. Bottom panel: Ratio of the two spectra shown in the top panel. The observed asymmetry is directly proportional to the residual polarization of positrons forming Ps; its amplitude ($\approx 2\epsilon P$) is indicative of the polarimeter's high analyzing power.

gion where the triplet decays dominate ($t \geq 4$ ns), the relationship between A and P is approximately given by

$$A(t) = N_+/N_- \approx 1 + 2\varepsilon P [(1 - \varepsilon P) + 2(\lambda/\lambda') \exp(\lambda' - \lambda)t]^{-1}, \quad (1)$$

where $\varepsilon = x(1+x^2)^{-1/2}$, $x = 0.0276|B|$ (in kG), and λ' (λ) is the inverse lifetime of the perturbed (unperturbed) triplet state.

The data of Fig. 1 were obtained with the system shown schematically in Fig. 2. The ^{10}C and ^{14}O were produced in the same target (140-mg/cm² BN enriched to 90% in ^{10}B) by (p, n) activation with 14.5-MeV protons of 6 μA . After irradiation, the target was transported to the spectrometer, which selected 1.22-MeV positrons with a momentum resolution of 12.5% FWHM and a transmission of 3%. Positrons entering the polarimeter field ($B = 9.5$ kG) sequentially cross a 0.4-nm-thick NE104 plastic START scintillator and 1.0-mm-thick beryllium moderator, and stop in a MgO powder pellet placed in vacuum. The powder, characterized by a grain

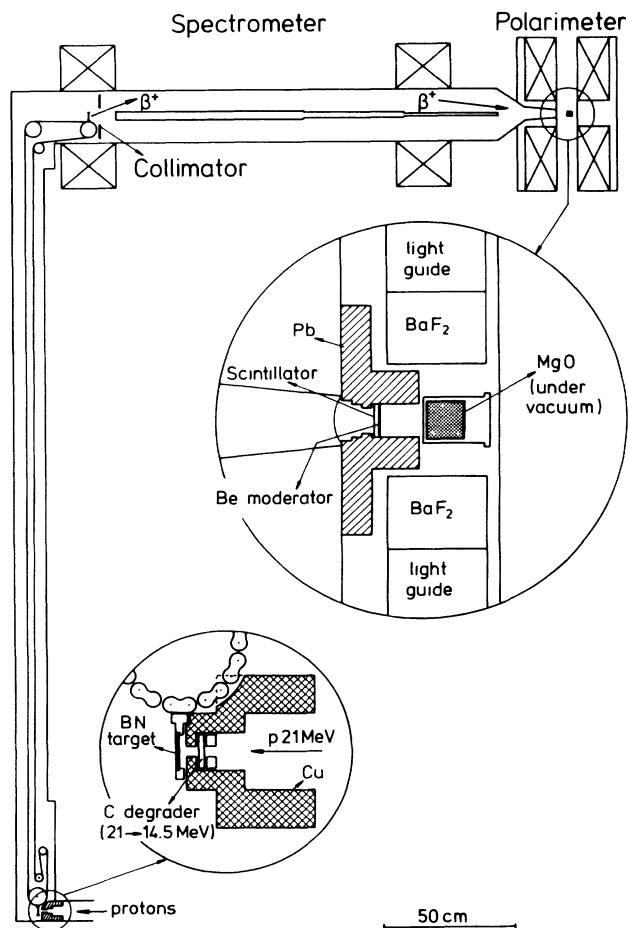


FIG. 2. The UCL on-line positron polarimeter system: activation site (small inset), target transport system, spectrometer, and polarimeter (large inset).

3250

diameter of about 100 Å, was compressed to 0.33 g/cm³ and heat treated at 300°C in vacuum for several hours in order to remove excess oxygen and water: The Ps formation fraction was 43%, and the unperturbed triplet lifetime was 4% less than its current experimental vacuum value.⁸ The decay and direct annihilation photons were observed by two 5.1-cm-diameter-by-3.8-cm BaF₂ STOP scintillators mounted in the polarimeter magnet housing at 180° to each other in a plane perpendicular to the field axis, with a 511-keV detection probability of 18%. A lead collimator, placed between the START and the STOP detectors (Fig. 2, inset), reduced the relative contribution of Ps photons formed in the START scintillator to 7×10^{-3} of the events in our time window of interest. Each STOP scintillator was coupled to a shielded XP2020Q photomultiplier located outside the polarimeter field region through a 30-cm quartz lightguide: The START scintillator was edge coupled with Lucite to a shielded XP2020 photomultiplier. Detector signals were processed by constant-fraction-timing discriminators without intermediate amplification. The two STOP channels were individually time aligned to within 15 ps of each other, and connected in OR logic to a time-to-digital converter of 156-ps channel width from which the time-resolved decay spectra were obtained. Timing calibration yielded a resolution of 1.3 ns (FWHM).

The simultaneous measurement of both decays is a unique aspect of this measurement. The fact that the relative contributions of F and GT decay positrons change with time following irradiation [$t_{1/2}(^{10}\text{C}) = 19.3$ s, $t_{1/2}(^{14}\text{O}) = 70.6$ s] allows a comparison of their polarizations. Measurements were performed in two kinds of cycles to nearly equalize the instantaneous detection rates of the two isotopes. The first, A (predominantly ^{10}C), consisted of a 50-s data-acquisition window following a 7-s target activation; the second, B (predominantly ^{14}O), consisted of a 200-s data-acquisition window following 70-s activation and 65-s wait. A sequence of one A and two B cycles was repeated with the polarimeter field reversed each two cycles: With twice more A cycles than B , the total statistics were similar in both acquisition windows. The β activity of the target seen by the START detector was recorded in 1-s steps by multiscalers in order to determine the relative contributions of ^{10}C and ^{14}O , which were resolved on the basis of their characteristic lifetimes. The $\beta\gamma$ trigger rate was simultaneously stored in 1-s steps in order to determine the total dead time during each cycle. Instantaneous β rates ranged from 696 to 186 kHz in window A , and from 768 to 86 kHz in window B . The system response function was measured every 8 h by replacing the powder target with a stack of beryllium foils of similar macroscopic density and dimensions.

Data were obtained with both Be and MgO over a total of 151 h: 123 h with MgO, and 28 h with Be. Each recorded $\beta\gamma$ time spectrum was corrected for accidental $\beta\gamma$ coincidences and appropriately summed to yield the

total decay spectra for each of the two magnetic-field directions in each window (*A* and *B*). From these, again for each window, we constructed the sum and the ratio spectra for both field directions. A fit was then made simultaneously to these four spectra, convoluting the complete theoretical Ps decay spectra⁷ with the measured response function, over a time region of 58.6 ns beginning 3.8 ns after the direct annihilation peak. This region was chosen to optimize the fitting precision with respect to the accidental contributions. The parameters assumed common to all spectra were the perturbed and unperturbed triplet lifetimes and the Ps formation fraction; those specific to each windows were, in addition to the polarization, the amplitude of the 2.5-ns component associated with Ps formation in the START scintillator. From these fits, we obtain $K = P_B/P_A = 1.0011 \pm 0.0020$ (stat).

The corrections and possible systematic errors are summarized in Table I. The largest correction arises from $t=0$ shifts in the location of the prompt peak between measurement cycles due to electronic instabilities, which can artificially generate asymmetries if not accounted for. These shifts were determined by fitting the ratio of the direct annihilation peaks by the ratio of two identical peaks shifted by a known amount, and amounted to a 2-ps difference between windows. The largest uncertainty contribution to the measurement, however, arises from a small ¹¹C contamination ($t_{1/2} = 20.4$ min) due to the 5% ¹¹B present in the enriched target, and to the ¹⁴N(p, α)¹¹C reaction: This contributed 1% of positrons in window *A* and 1.8% in window *B* despite a spectrometer setting above the ¹¹C spectrum end point (0.96 MeV). Their polarization was measured in a separate experiment using a natural BN target (80% ¹¹B).

There are three types of accidental by coincidences: (a) uncorrelated background, which is observed at "negative" times, (b) coincidences in which the observed γ comes from a β which precedes the β START, which are electronically rejected, and (c) coincidences wherein the observed γ is emitted by a β which penetrated the powder after the β START. The last were carefully estimated on the basis of β rate, $\beta\gamma$ rate, and the rate of β detected after the β START in a well-defined temporal window, and the uncertainty estimate checked experi-

mentally.

Differential depolarization of the decay positrons was minimized by their simultaneous activation in the same BN target. Differences between *A* and *B* window measurements, due to the different spatial distribution of ¹⁰C and ¹⁴O in the target, were determined in a separate measurement of the relative ¹⁰B(p, n)¹⁰C and ¹⁴N(p, n)¹⁴O cross sections for proton energies between 10 and 14.5 MeV. Positron depolarization in BN as a function of target thickness was measured by observing the residual polarization of positrons emitted by a ⁶⁸Ga source sandwiched between BN foils of thickness ranging from 0 to the total target width of 140 mg/cm². The internal surfaces of the spectrometer were covered with rough-surfaced low-*Z* material in order to minimize any differential wall-scattering depolarization resulting from the difference in the β -spectrum end points of the two isotopes. Differential depolarization on stopping, due to the 3% difference in the ¹⁰C/¹⁴O β -spectrum end points, was evaluated using the approach of Bouchiat and Levy-Leblond,⁹ and tested by measuring the residual polarization of positrons emitted by ⁶⁸Ga for selected energies ranging from 770 to 1260 keV.

The polarization comparison between windows *A* and *B*, after corrections, is $K = 0.9998 \pm 0.0021$. Accounting for the fact that each window polarization is a combination of ¹⁰C and ¹⁴O polarizations ($P_A = 0.728P_{GT} + 0.272P_F$, $P_B = 0.176P_{GT} + 0.833P_F$), we then obtain $R = 0.9996 \pm 0.0037$. This result further includes a small contribution of positrons from ¹⁵N(p, n)¹⁵O. Not included is a correction¹⁰ which arises from weak magnetism in ¹⁰C decay. This is related to the width of the radiative analog *M*1 transition in ¹⁰B by the conserved-vector-current hypothesis, and yields¹¹ a negligible correction of 3×10^{-4} to R ; the sign is, however, indeterminate.

Our final result is comparable with that of the Groningen group, and with a recent experiment in ²⁶Al/²⁵Al using a similar Ps-based technique.¹² For minimal parity symmetric extensions of the standard model, $R = 1 + 8\zeta\delta$, where ζ is the mixing angle and δ is the mass-squared ratio of left- and right-handed *W* bosons,¹ and our result implies $-8.1 < \zeta\delta \times 10^4 < 7.1$ (90% C.L.). The weighted average of all three results yields $-4.0 < \zeta\delta \times 10^4 < 7.0$ (90% C.L.): This average constitutes the best limit on right-handed-current contributions to the weak interaction derived from β polarization experiments to date, and is shown in Fig. 3 in comparison with other results obtained from pure leptonic and semi-leptonic sectors.

In the absence of right-handed currents, and neglecting time-reversal violation, our result limits possible scalar-tensor-current admixtures to $C_S/C_V - 1.001(C_T/C_A) = -0.0007 \pm 0.0105$ (90% C.L.). Combined with the Groningen result, $C_S/C_V - C_T/C_A = 0.0014 \pm 0.0090$ (90% C.L.). This bound is complementary to recent limits of $C_S/C_V = (0.6 \pm 4.1) \times 10^{-3}$ (90% C.L.) deduced

TABLE I. Systematic corrections to the measured polarization ratio $K = P_B/P_A$.

Accidental coincidences	$(-0.14 \pm 0.02) \times 10^{-3}$
Timing shifts	$(-0.95 \pm 0.14) \times 10^{-3}$
¹¹ C contribution	$(+0.23 \pm 0.61) \times 10^{-3}$
¹⁰ C/ ¹⁴ O target-depth difference:	
depolarization in target	$(-0.07 \pm 0.02) \times 10^{-3}$
¹⁰ C/ ¹⁴ O end-point difference:	
stopping depolarization	$(-0.43 \pm 0.08) \times 10^{-3}$
Total	$(-1.36 \pm 0.63) \times 10^{-3}$

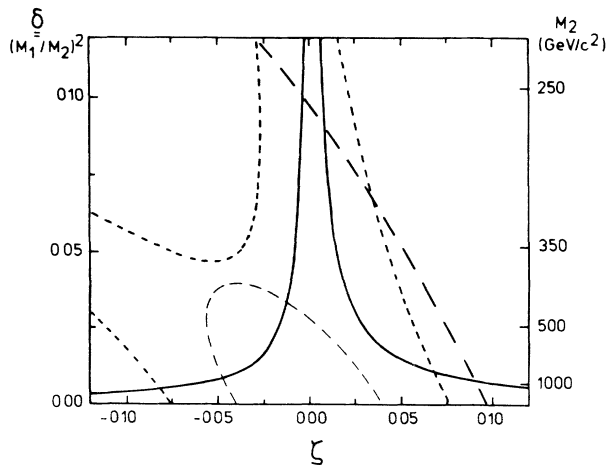


FIG. 3. Constraints, at 90% confidence, on the parameter $\delta = (M_1/M_2)^2$ and the mixing angle ζ deduced from the world average (this work and Refs. 5 and 12) in relative polarization measurements (bold line), and from other semileptonic experiments: β polarization measurements (Ref. 16) (bold dashed line) and neutron-decay measurements (Ref. 17) (bold short-dashed line). Also shown is the bound from the measurement of e^+ end point in muon decay (Ref. 18) (dashed line).

from $0^+ - 0^+$ transitions,¹³ and $C_T/C_A = (-3 \pm 8) \times 10^{-4}$ (68% C.L.) from a least-squares analyses of nuclear β -decay data.¹⁴

While a significant aspect of this measurement is its demonstrated statistical power, a substantial increase is still required before precisions better than 0.1% in reasonable counting times can be foreseen. This is possible through an increase in subtended solid angle of the STOP detection system, and improved timing resolution. At the present level, however, additional correlation measurements of positron polarization in the decays of polarized nuclei become possible which offer an order-of-magnitude improvement in their sensitivity to δ .¹⁵ These are currently being pursued.

We have appreciated many useful discussions with M. Skalsey and J. van Klinken during the evolution of this

measurement, and with B. Holstein on some aspects of the analysis. We gratefully acknowledge the numerous contributions of the University Catholique de Louvain (UCL) cyclotron, mechanical, and electronic staff, without whom this work could not have been accomplished. We also thank M. Jacques, B. Tasiaux, D. Claes, L. Michel, F. Vecchio Verderame, and D. Dedouaire for their assistance during various phases of the work. This project was supported by the Belgian Fund for Scientific Research.

(a)Temporarily at University of South Carolina, Columbia, SC 29208.

¹P. Herczeg, in *Weak and Electromagnetic Interactions in Nuclei*, edited by H. V. Klapdor (Springer-Verlag, Heidelberg, 1986), p. 528, and references therein.

²J. D. Jackson *et al.*, Nucl. Phys. **4**, 206 (1957).

³P. Langacker and S. U. Sankar, Phys. Rev. D **40**, 1569 (1989).

⁴R. Barbieri and R. N. Mohapatra, Phys. Rev. D **39**, 1229 (1989).

⁵V. A. Wichers *et al.*, Phys. Rev. Lett. **58**, 1821 (1987).

⁶M. Skalsey, T. A. Girard, D. Newman, and A. Rich, Phys. Rev. Lett. **49**, 708 (1982); M. Skalsey *et al.*, Phys. Rev. C **32**, 1014 (1985).

⁷T. A. Girard *et al.*, Z. Phys. A **330**, 51 (1988).

⁸S. Orito *et al.*, Phys. Rev. Lett. **63**, 597 (1989).

⁹C. Bouchiat and J. M. Levy-Leblond, Nuovo Cimento **23**, 193 (1963).

¹⁰B. R. Holstein, Phys. Rev. C **16**, 1258 (1977); T. A. Girard, Phys. Rev. C **27**, 2418 (1983).

¹¹F. P. Calaprice and B. R. Holstein, Nucl. Phys. **A273**, 301 (1976); **A490**, 144 (1988).

¹²M. Skalsey *et al.*, Phys. Rev. C **39**, 986 (1989).

¹³W. E. Ormand *et al.*, Phys. Rev. C **40**, 2814 (1989).

¹⁴A. I. Boothroyd *et al.*, Phys. Rev. C **29**, 603 (1984).

¹⁵P. A. Quin and T. A. Girard, Phys. Lett. B **229**, 29 (1989).

¹⁶J. Van Klinken *et al.*, Phys. Rev. Lett. **50**, 94 (1983).

¹⁷D. Dubbers *et al.*, Europhys. Lett. **11**, 195 (1990).

¹⁸A. Jodidio *et al.*, Phys. Rev. D **34**, 1967 (1986); **37**, 237(E) (1988).

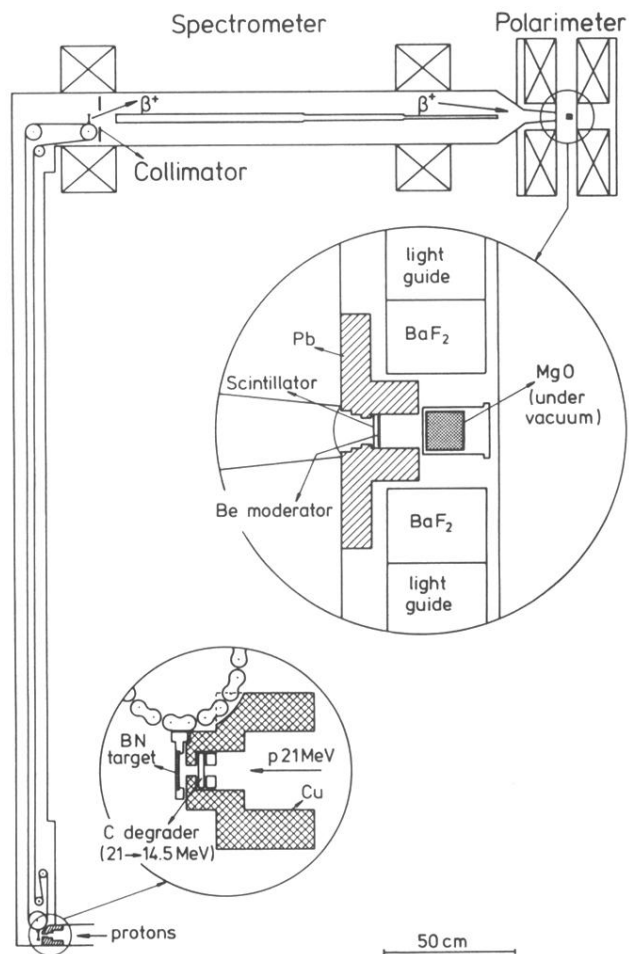


FIG. 2. The UCL on-line positron polarimeter system: activation site (small inset), target transport system, spectrometer, and polarimeter (large inset).